Polymers as compressible soft spheres

Giuseppe D'Adamo*

Dipartimento di Fisica, Università dell'Aquila,

V. Vetoio 10, Loc. Coppito, I-67100 L'Aquila, Italy

Andrea Pelissetto†

Dipartimento di Fisica, Sapienza Università di Roma and INFN,

Sezione di Roma I, P.le Aldo Moro 2, I-00185 Roma, Italy

Carlo Pierleoni‡

[3] *Dipartimento di Fisica, Università dell'Aquila and CNISM,*

UdR dell'Aquila, V. Vetoio 10, Loc. Coppito, I-67100 L'Aquila, Italy

Abstract

We consider a coarse-grained model in which polymers under good-solvent conditions are represented by soft spheres whose radii, which should be identified with the polymer radii of gyrations, are allowed to fluctuate. The corresponding pair potential depends on the sphere radii. This model is a single-sphere version of the one proposed in Vettorel *et al.*, Soft Matter **6**, 2282 (2010), and it is sufficiently simple to allow us to determine all potentials accurately from full-monomer simulations of two isolated polymers (zero-density potentials). We find that in the dilute regime (which is the expected validity range of single-sphere coarse-grained models based on zero-density potentials) this model correctly reproduces the density dependence of the radius of gyration. However, for the thermodynamics and the intermolecular structure, the model is largely equivalent to the simpler one in which the sphere radii are fixed to the average value of the radius of gyration and radii-independent potentials are used: for the thermodynamics there is no advantage in considering a fluctuating sphere size.

PACS numbers: 61.25.he, 82.35.Lr

I. INTRODUCTION

Polymer solutions are very interesting soft-matter systems, showing a wide variety of behaviors, depending on density, temperature, architecture, etc.[1–4] Due to the large number of atoms belonging to a single macromolecule, simulations of polymer systems are quite challenging. For this reason, during the years many attempts have been made to develop coarse-grained (CG) models in which only some *relevant* degrees of freedom are retained, in such a way to reproduce some large-scale structural properties and the thermodynamic behavior.[5] In the simplest approach one maps polymer chains onto point particles interacting by means of the pairwise potential of mean force between the centers of mass of two *isolated* polymers.[5–8] Since the potentials are computed in the limit of zero polymer density, this approach is limited to the dilute regime, in which many-body interactions[9,10] can be neglected. This limitation was overcome ten years ago,[11,12] by introducing pair potentials depending on the polymer density, thus allowing the model to reproduce exactly the thermodynamics at any given density. This work has paved the way to the use of soft effective particles to represent polymer coils in complex situations such as in modelling colloid-polymer mixtures.[13] However, deriving density-dependent potentials requires full-monomer simulations at finite polymer density, which is what one would like to avoid by using CG models. Moreover, care is needed to derive the correct thermodynamics[14–16] and to compute free energies and phase diagrams.[5]

These limitations can be overcome by switching to a model at a lower level of coarse graining, i.e. by mapping a long linear polymer to a short linear chain of soft effective blobs.[17–23] Quite recently, extending an older phenomenological approach,[24,25] Ref. 21 proposed a multiblob model. As in the models proposed in Refs. 17,19,22,23, the potentials do not depend on polymer density and are fixed by using structural data obtained in the limit of zero polymer density. However, at variance with the other approaches, the radius of each blob, which should be identified with its radius of gyration, is not fixed but is allowed to fluctuate. The idea is very appealing and the model is, in principle, more realistic, since blobs are compressible: when the density increases, the average blob radius of gyration decreases as it does in the original polymer model. Therefore, this model should provide a more accurate description of the structural properties of the polymers. However, its practical implementation is by no means straightforward. A phenomenological approach was proposed

in Ref. 21, in which intermolecular and intramolecular potentials appropriate for polymers under good-solvent conditions were determined by combining exact results for ideal chains and some approximate predictions for good-solvent polymers that allowed the inclusion of the local self-repulsion.

In this paper, we wish to test the approach of Ref. 21 for polymers under good-solvent conditions. We consider a single-blob system and carefully compare the results obtained for the model with radii-dependent potentials with those obtained for the simpler model in which the blob size is fixed. The simplicity of the CG single-blob model allows us to compute the pair potentials from full-monomer simulations of two isolated chains, avoiding any approximation, thus allowing us to distinguish between the merits/demerits of the method from those of the approximations which are needed to implement it. Moreover, we can discuss two different approaches to the coarse graining: in the first one each polymer is represented by a soft "compressible" sphere located in the polymer center of mass (this is the most common approach when dealing with linear polymers); in the second one the position of the sphere coincides with that of the central monomer (star-polymer studies favor this second option).

The paper is organized as follows. In Sec. II we define the models we investigate. In Sec. III we present our results: in Sec. III A we discuss the third virial coefficient and the zero-density three-body forces, while in Sec. III B we compare the results for the compressibility factor, the center-of-mass (or polymer midpoint) pair distribution function, and the distribution of the radius of gyration in the semidilute regime. Finally, in Sec. IV we present our conclusions.

II. THE MODELS

In this paper polymers are represented as "compressible" soft spheres of radius σ: two spheres of radii σ_1 and σ_2, respectively, interact by means of the pair potential $V(\sigma_1, \sigma_2; b)$, where b is the relative distance. The radius of each sphere is allowed to fluctuate. We assume that the normalized radius distribution for an isolated sphere is given by the function $P(\sigma)$.

For a system of L spheres in a volume V, we consider the partition function

$$Z = \int d\sigma_1 P(\sigma_1) \dots d\sigma_L P(\sigma_L) Q_L(\sigma_1, \dots, \sigma_L)$$
$$Q_L(\sigma_1, \dots, \sigma_L) = \int_V d^3\boldsymbol{b}_1 \dots d^3\boldsymbol{b}_L \, \exp\left[-\beta \sum_{i>j} V(\sigma_i, \sigma_j; b_{ij})\right], \tag{1}$$

where $\boldsymbol{b}_i$ is the position of the i-th sphere and $b_{ij} = |\boldsymbol{b}_i - \boldsymbol{b}_j|$. Equivalently, as in Ref. 21, we can define a potential $\beta V_1(\sigma) = -\ln P(\sigma)$ and write the partition function as

$$Z = \int d\sigma_1 d^3\boldsymbol{b}_1 \dots d\sigma_L d^3\boldsymbol{b}_L \, \exp\left[-\beta \sum_i V_1(\sigma_i) - \beta \sum_{i>j} V(\sigma_i, \sigma_j; b_{ij})\right]. \tag{2}$$

The distribution $P(\sigma)$ as well as the potentials $V(\sigma_1, \sigma_2; b)$ are determined in such a way to reproduce the thermodynamics and the intermolecular spatial distribution of the polymers in the limit of zero polymer density. More specifically, we consider a polymer model, in which each polymer consists of N monomers located in $\mathbf{r}_1, \dots \mathbf{r}_N$. As usual we define the radius of gyration of the chain as

$$r_g^2 = \frac{1}{2N^2} \sum_{ij} (\mathbf{r}_i - \mathbf{r}_j)^2, \tag{3}$$

and its average over all polymer configurations as $R_g^2(N) = \langle r_g^2 \rangle$. We indicate zero-density averages with a hat, so that $\hat{R}_g(N)$ is the average radius of gyration of a single isolated polymer. It is a function of N and for $N \to \infty$ (scaling limit) it scales as

$$\hat{R}_g(N) = aN^\nu (1 + bN^{-\Delta} + \dots), \tag{4}$$

where a and b are model-dependent constants and ν and Δ are universal exponents. For good-solvent polymers they are known quite precisely:[26] $\nu = 0.587597(7)$, $\Delta = 0.528(12)$. To define $P(\sigma)$ we consider the distribution of the radius of gyration of an isolated polymer,

$$Q(s; N) = \langle \delta(r_g - s) \rangle_1, \tag{5}$$

where $\langle \cdot \rangle_1$ is the statistical average over all the conformations of an isolated polymer made of N monomers. In the scaling limit $N \to \infty$, the adimensional quantity $\hat{R}_g(N) Q(s; N)$ is a universal function of $\sigma = s/\hat{R}_g$, which we identify with $P(\sigma)$:

$$\hat{R}_g(N) Q(s; N) = P(\sigma) + O(N^{-\Delta}). \tag{6}$$

Scaling corrections decay as $N^{-\Delta}$, where Δ is the same universal correction-to-scaling exponent appearing in Eq. (4). The function $P(\sigma)$ satisfies

$$\int d\sigma\, P(\sigma) = 1, \qquad \int d\sigma\, \sigma^2 P(\sigma) = 1, \tag{7}$$

the second equation being a direct consequence of the definition of $\hat{R}_g$. To define the potential, we first consider the model in which the CG spheres are located in the centers of mass of the polymers. In this case we first consider

$$\beta v(s_1, s_2; r; N) = -\ln \frac{\langle e^{-\beta U_{\rm interm}} \delta(r_{g,1} - s_1)\delta(r_{g,2} - s_2)\rangle_{\mathbf{0},\mathbf{r}}}{Q(s_1; N)Q(s_2; N)}, \tag{8}$$

where the average $\langle\cdot\rangle_{\mathbf{0},\mathbf{r}}$ is over all isolated polymer pairs made of N monomers, such that their centers of mass are in the origin $\mathbf{0}$ and in $\mathbf{r}$, respectively, $r_{g,1}$ and $r_{g,2}$ are the gyration radii of the two polymers, and $U_{\rm interm}$ is the intermolecular interaction energy. In the scaling limit $N \to \infty$, $v(s_1, s_2; r; N)$ converges to a universal function, which we identify with the pair potential of the CG model:

$$v(s_1, s_2; r; N) = V(\sigma_1, \sigma_2; b) + O(N^{-\Delta}), \tag{9}$$

where $\sigma_1 = s_1/\hat{R}_g$, $\sigma_2 = s_2/\hat{R}_g$, and $b = r/\hat{R}_g$. Because of these definitions, the polymer center-of-mass pair distribution function in the limit of zero polymer density is the same as the zero-density pair distribution function between the centers of the spheres. Hence, the polymer thermodynamics is correctly reproduced in the low-density limit by the effective model.

It is important to stress that the quantities $P(\sigma)$ and $V(\sigma_1, \sigma_2; b)$ are *universal*, i.e. the same result is obtained by using any model that is appropriate to describe polymers under good-solvent conditions. One could use the well-known lattice self-avoiding walk model or any off-lattice model appropriate to describe good-solvent polymers, for instance the bead-rod model of Ref. 21. We will use the lattice Domb-Joyce model with $w = 0.505838$ (see Ref. 27 for details on the model). In the scaling limit $N \to \infty$ such a model describes polymers under good-solvent conditions. Morever, for our particular choice of the parameter w, the scaling corrections proportional to $N^{-\Delta}$ that appear in Eqs. (6) and (9) are very small, so that we can obtain the asymptotic (scaling) functions $P(\sigma)$ and $V(\sigma_1, \sigma_2; b)$ from simulations of chains of moderate length. The results we shall present are obtained by using chains with $N = 600$. We have also performed simulations with $N = 2400$: the

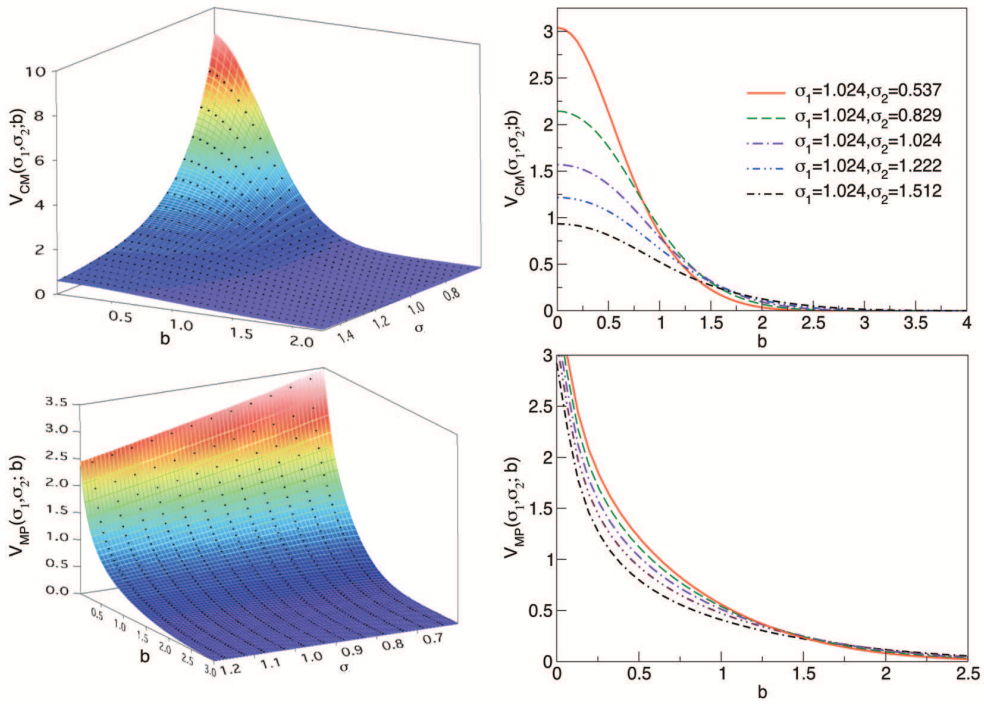

FIG. 1: On top we report the center-of-mass potentials $\beta V(\sigma_1, \sigma_2; b)$: on the left we show a three-dimensional plot in terms of $\sigma = \sigma_1 = \sigma_2$ and $b = r/\hat{R}_g$, on the right we show the potentials for $\sigma_1 = 1.024$ and several values of σ_2, as a function of b. On bottom we show the same plots for the midpoint potentials $V_{MP}(\sigma_1, \sigma_2; b)$.

corresponding results are fully compatible with those obtained using $N = 600$, indicating the absence of relevant finite-length effects. In practice, we simulate two independent Domb-Joyce chains using the highly-efficient pivot algorithm[28] (we perform 1.25×10^9 pivot trial moves on each of them) and determine numerically $Q(s, N = 600)$ and $v(s_1, s_2; r; N = 600)$. Then, we define $P(\sigma) = \hat{R}_g(N = 600)Q(s, N = 600)$ and $V(\sigma_1, \sigma_2; b) = v(s_1, s_2; r; N = 600)$, with $s = \sigma\hat{R}_g(N = 600)$ (analogous relations hold for s_1 and s_2) and $r = b\hat{R}_g(N = 600)$. Plots of the potential for several values of σ_1 and σ_2 are reported in Fig. 1. They have an approximately Gaussian behavior with $V(\sigma_1, \sigma_2; b = 0)$ increasing as the radii decrease. This is of course expected, since the smaller σ_1 and σ_2 are, the more compact the two walks become. Hence repulsion should increase. For the same reasons, the range of the potentials decreases as the radii decrease.

In Ref. 21, on the basis of a heuristic argument, it was suggested that the pair potentials could be approximately written as

$$V_{VBK}(\sigma_1,\sigma_2;b) = \epsilon(\sigma_1^2+\sigma_2^2)^{-3/2}\exp\left(-\alpha\frac{b^2}{\sigma_1^2+\sigma_2^2}\right), \tag{10}$$

where $\alpha = 3/2$ and ϵ is a constant independent of σ_1 and σ_2. We find that this expression works reasonably well when taking $\epsilon \approx$ 4-5. To obtain an optimal approximation we determine α and ϵ in such a way to minimize the functional

$$\Psi(\alpha,\epsilon) = \int_0^\infty d\sigma_1 \int_0^\infty d\sigma_2 \int_0^{b_{\max}} db \left[P(\sigma_1)P(\sigma_2)b^2\left(e^{-\beta V(\sigma_1,\sigma_2;b)} - e^{-\beta V_{VBK}(\sigma_1,\sigma_2;b)}\right)\right]^2, \tag{11}$$

where $V(\sigma_1,\sigma_2;b)$ and $P(\sigma)$ are the quantities computed from full-monomer simulations. Since the Monte Carlo estimates of V for $b \gtrsim 3$ are noisy, we excluded these values from the b integration, taking $b_{\max} = 3$. The functional (11) has been chosen on the basis of the expression of the second-virial universal combination[29]

$$A_2 = 2\pi \int d\sigma_1 d\sigma_2 db P(\sigma_1)P(\sigma_2)b^2\left(1 - e^{-\beta V(\sigma_1,\sigma_2;b)}\right). \tag{12}$$

We obtain

$$\alpha = 1.42, \qquad\qquad \epsilon = 4.42. \tag{13}$$

Note that the optimal value for α is quite close to the value $\alpha = 3/2$ proposed in Ref. 21. In Fig. 2 we plot $(\sigma_1^2+\sigma_2^2)^{3/2}V(\sigma_1,\sigma_2;b)$ vs $R = b(\sigma_1^2+\sigma_2^2)^{-1/2}$ for several values of σ_1 and σ_2. The results are then compared with the phenomenological expression $\epsilon\, e^{-\alpha R^2}$, obtained using potential (10). We observe reasonable agreement for $R \gtrsim 1$, while significant discrepancies are observed for $R \to 0$. However, this is exactly the region which does not contribute significantly to A_2, hence to the thermodynamics.

Up to now we have characterized the polymer position by using its center of mass: in definition (9) b represents the distance between the two centers of mass, expressed in units of $\hat{R}_g$: $b = r/\hat{R}_g$. This is the usual choice for CG models of linear polymers. On the other hand, when considering star polymers, it is much more common to consider CG models in which the star position is identified with the position of the ramification point, the center of the star.[5,30–33] If we view linear polymers as two-arm star polymers, it is natural to define the CG model using the central monomer as polymer position. In an exact mapping this choice would be ininfluential for the thermodynamics.[5] However, since all n-polymer interactions with $n \geq 3$ are neglected in the CG model, different choices of the point associated with the

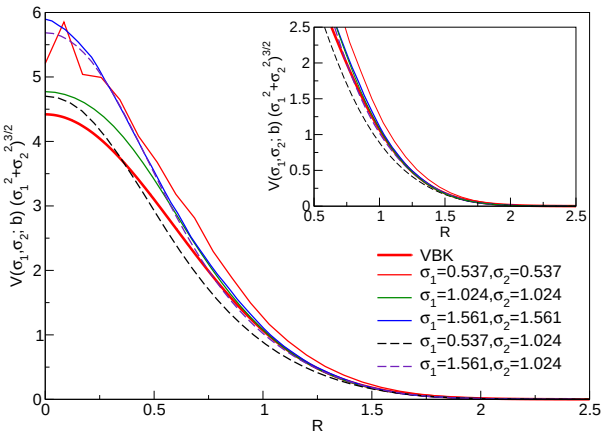

FIG. 2: Rescaled potentials $(\sigma_1^2+\sigma_2^2)^{3/2}V(\sigma_1,\sigma_2;b)$ as a function of $R=b(\sigma_1^2+\sigma_2^2)^{-1/2}$ for several values of σ_1 and σ_2. We also plot the function $\epsilon\, e^{-\alpha R^2}$, with $\epsilon=4.42$, $\alpha=1.42$ (VBK).

polymer position give rise to CG models with different thermodynamic behavior. It makes therefore sense to study the different possibilities, with the purpose of understanding which is the optimal one.

We thus also study two different CG models in which the polymer position is given by the central monomer $\mathbf{r}_{N/2}$. We consider a model in which polymers are represented by identical spheres interacting by means of the potential of mean force

$$V_{MP}(b) = -\ln\langle e^{-\beta U_{\rm interm}}\rangle_{\mathbf{0},\mathbf{r}}, \tag{14}$$

where now the average is over all isolated polymer pairs such that the central monomers (midpoints, MP) are in the origin and in $\mathbf{r}$, respectively, and $b=r/\hat{R}_g$. We also consider the model with compressible soft polymers interacting by means of the potential $V_{MP}(\sigma_1,\sigma_2;b)$ defined as in Eq. (9), where now b is the distance between the central monomers expressed in units of $\hat{R}_g$.

The potential $V_{MP}(b)$ has been discussed at length in the context of star polymers. For $b\to 0$ it diverges logarithmically as[34] $\ln(1/b)$. An explicit parametrization has been given in Ref. 35 (see their results for a two-arm star polymer):

$$V_{MP}(b) = \frac{1}{\tau}\ln\left[\left(\frac{\alpha}{b}\right)^{\tau\beta} e^{-\delta b^2} + \exp(\tau\gamma e^{-\delta b^2})\right], \tag{15}$$

where

$$\alpha=1.869,\ \beta=0.815,\ \gamma=0.372,\ \delta=0.405,\ \tau=4.5. \tag{16}$$

This parametrization is quite precise. For instance, we obtain 5.51 for the second-virial combination A_2, which is very close to the polymer result[27] $A_2 = 5.500(3)$.

In the bottom panels of Fig. 1 we report the potential $V_{MP}(\sigma_1, \sigma_2; b)$. It is interesting to observe that they all diverge logarithmically as $b \to 0$, apparently with the same type of logarithmic behavior, $V_{MP}(\sigma_1, \sigma_2; b) \sim 0.82 \ln(1/b)$, for all values of σ_1 and σ_2.

III. COMPARISON OF THE MODELS

In this section we compare the thermodynamic behavior of the models we have introduced in the previous section:

a) the standard CG model in which polymers are identical soft spheres interacting with a potential which only depends on distance. We consider the case in which the polymer position is given by the position of the center of mass (model M1a) or of the central monomer (model M1b). In the first case we use the accurate expression of the pair potential[36] given in Ref. 37, in the second one we use Eq. (15) with parameters (16).

b) We consider the "compressible" CG model in which we use either the center of mass (model M2a) or the central monomer (model M2b) as polymer position. We also consider the model with pair potential (10) with parameters given by (13) (model M2c).

The results will be compared with full-monomer results and, for comparison, with those obtained in the tetramer model (results will be labelled with "t") introduced recently in Ref. 22.

A. Three-body interactions at zero density

If we expand the compressibility factor in powers of the concentration $c = L/V$ as

$$Z = \frac{\Pi}{k_B T c} = 1 + B_2 c + B_3 c^2 + O(c^3), \tag{17}$$

the quantity $A_2 = B_2/\hat{R}_g^3$ is universal. An accurate estimate is[27] $A_2 = 5.500(3)$. Since we have matched the center-of-mass or polymer-midpoint distribution function to determine the pair potential, all models should give the correct estimate of the combination A_2. In

TABLE I: Virial-coefficient universal combinations for the models introduced in Sec. III and for the tetramer model (t) of Ref. 22. We also report the universal asymptotic values for polymers (p).[27]

	p	M1a	M1b	M2a	M2b	M2c	t
A_2	5.500(3)	5.4926(1)	5.5109(1)	5.5102(3)	5.5085(2)	5.5738(3)	5.597(1)
A_3	9.80(2)	7.844(6)	4.925(4)	7.42(2)	4.43(2)	7.22(2)	9.99(2)
A_3'	10.64	7.844(6)	4.925(4)	8.015(5)	5.012(2)	7.809(5)	10.57(2)
$A_{3,fl}$	−0.84	0	0	−0.59(2)	−0.58(2)	−0.58(2)	−0.581(5)

Table I we report the results for the models we consider. Differences are small, and are representative of the level of precision with which the models reproduce the polymer center-of-mass or midpoint distribution function. Note that the estimate corresponding to model M2c is very close to the correct one, indicating that expression (10) parametrizes quite accurately the R_g dependence of the potentials.

Much more interesting is the comparison of the third virial coefficient, since it provides an indication of the accuracy with which the CG models reproduce the polymer thermodynamics in the dilute regime and also of the importance of the three-body forces which have been neglected. The universal combination $A_3 = B_3/\hat{R}_g^6$ was computed in Ref. 27 finding

$$A_3 = 9.80(2). \tag{18}$$

In order to determine A_3, two contributions had to be computed. One contribution is the standard one, which is the only one present in monoatomic fluids and in fluids of rigid molecules, $A_3' \approx 10.64$, while the second one is a flexibility contribution $A_{3,fl} \approx -0.84$ (it corresponds to $-T_1\hat{R}_g^{-6}$ in the notations of Ref. 27). The combination A_3 as well as the two contributions A_3' and $A_{3,fl}$ are universal, hence it makes sense to compare them with the corresponding results in the CG models.

We have estimated A_3 for all models. The results are reported in Table I. Note that, while $A_{3,fl}$ vanishes in models M1a and M1b, a nonvanishing contribution with the correct sign is obtained for the models with a fluctuating radius. On the other hand, the estimates of A_3 for models with radii-dependent potentials are essentially equivalent to those in which the sphere radii are fixed: the estimates corresponding to models M2a and M2b are close to those of models M1a and M1b, respectively. To be precise, discrepancies increase by

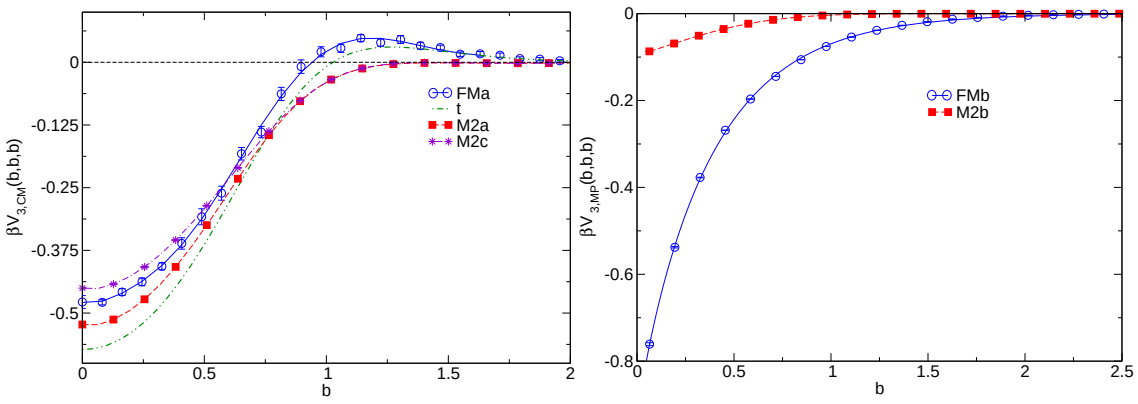

FIG. 3: Three-body potential of mean force $\beta V_3(\mathbf{r}_{12}, \mathbf{r}_{13}, \mathbf{r}_{23})$ for $r_{12} = r_{13} = r_{23} = r$, as a function of $b = r/\hat{R}_g$. On the left we report results for models M2a, M2c, for the tetramer model (t) of Ref. 22, and the predictions of full-monomer simulations for the quantity associated with the center of mass (FMa); on the right we report the results for model M2b and the prediction of full-monomer simulations for the analogous quantity associated with the polymer midpoint (FMb).

allowing the radii to fluctuate: the difference between the M2a (or M2b) estimate of A_3 and the asymptotic polymer result is larger than the discrepancy observed for model M1a (or M1b, respectively). We can also compare the results for models M2a and M2c: the difference between the two estimates of A_3 is small, confirming that expression (10) is reasonably accurate. Finally, the results show that the CG models in which the center of mass is taken as reference point are more accurate than those in which the central monomer is considered. In the latter case, A_3 is underestimated by approximately a factor of two.

As a further check we compute the effective three-body potential of mean force defined by[10,37]

$$\beta V_3(\boldsymbol{b}_{12}, \boldsymbol{b}_{13}, \boldsymbol{b}_{23}) = -\ln \frac{\langle e^{-\beta U_{12}-\beta U_{13}-\beta U_{23}}\rangle_{\mathbf{b}_{12},\mathbf{b}_{13},\mathbf{b}_{23}}}{\langle e^{-\beta U_{12}}\rangle_{\mathbf{b}_{12}}\langle e^{-\beta U_{13}}\rangle_{\mathbf{b}_{13}}\langle e^{-\beta U_{23}}\rangle_{\mathbf{b}_{23}}}; \tag{19}$$

here U_{ij} is the intermolecular potential energy between molecules i and j and the average $\langle\cdot\rangle_{\mathbf{b}_{12},\mathbf{b}_{13},\mathbf{b}_{23}}$ is over the radii distributions of triplets of isolated spheres such that $\mathbf{b}_{ij} = \mathbf{b}_i - \boldsymbol{b}_j$, where $\boldsymbol{b}_i$ is the position of sphere i. In models M1a and M1b, the sphere radius does not fluctuate, so that $\langle e^{-\beta U_{ij}}\rangle_{\mathbf{b}_{ij}} = e^{-\beta V(b_{ij})}$ and $\langle e^{-\beta U_{12}-\beta U_{13}-\beta U_{23}}\rangle_{\mathbf{b}_{12},\mathbf{b}_{13},\mathbf{b}_{23}} = e^{-\beta V(b_{12})-\beta V(b_{13})-\beta V(b_{13})}$. It follows that $V_3(\boldsymbol{b}_{12}, \boldsymbol{b}_{13}, \boldsymbol{b}_{23}) = 0$. For models M2a, M2b, and M2c the average is over the distribution $P(\sigma)$ and U_{ij} should be identified with $V(\sigma_i, \sigma_j; b_{ij})$. Potential (19) should be compared with the analogous polymer quantity in which $\langle\cdot\rangle_{\mathbf{b}_{12},\mathbf{b}_{13},\mathbf{b}_{23}}$ is

the average over all conformations of triplets of isolated polymers such that $\boldsymbol{b}_i$ is the position (in units of $\hat{R}_g$) of the center of mass of polymer i (this is the case relevant for models M1a, M2a, and M2c) or the position of the polymer midpoint (the relevant potential for models M1b and M2b). The polymer three-body potential of mean force is universal in the scaling limit, i.e. it is model independent.

We computed $\beta V_3(\boldsymbol{b}_{12}, \boldsymbol{b}_{13}, \boldsymbol{b}_{23})$ for equilateral triangular configurations such that $b_{12} = b_{13} = b_{23} = b$ for models M2a and M2b. The results are reported in Fig. 3 and compared with the corresponding quantities (FMa and FMb) computed in full-monomer simulations. They were obtained by considering triplets of Domb-Joyce walks made of $N = 600$ beads. We used the pivot algorithm and performed 2.5×10^8 pivot trial moves on each of them. We also performed simulations with $N = 2400$, verifying the absence of finite-length effects.

For model M2a, we find $\beta V_3(b, b, b) = 0$ for $b \gtrsim 1.2$: for these values of b, model M2a is not different from the simpler model M1a. In particular, it does not reproduce the repulsive maximum that occurs for $b \approx 1.2$. On the other hand, model M2a appears to reproduce quite well the attractive short-distance part of $\beta V_3(b, b, b)$. The fact that model M2a gives a better estimate of $\beta V_3(b, b, b)$ than model M1a, while, at the same time, providing a slightly less accurate estimate of A_3 may seem contradictory at first sight. To understand it, let us note that (see Appendix for the derivation)

$$A_{3,\mathrm{pol}} - A_{3,CG} = -\frac{1}{3} \int d^3\boldsymbol{b}_{12} d^3\boldsymbol{b}_{13} \left(e^{-\beta V_{3,\mathrm{pol}}(\mathbf{b}_{12},\mathbf{b}_{13},\mathbf{b}_{23})} - e^{-\beta V_{3,\mathrm{CG}}(\mathbf{b}_{12},\mathbf{b}_{13},\mathbf{b}_{23})} \right) \times g(b_{12}) g(b_{13}) g(b_{23}), \tag{20}$$

where the subscripts "pol" and "CG" refer to the polymer and the CG model, respectively, and $g(b)$ is the zero-density center-of-mass pair distribution function, which is, by definition, identical in the polymer and in the CG model. Since $g(b)$ is small for small values of b, keeping also into account that $d\boldsymbol{b}_{12} d\boldsymbol{b}_{13}$ gives a factor $b_{12}^2 b_{13}^2$, the small-distance behavior of $V_3(\boldsymbol{b}_{12}, \boldsymbol{b}_{13}, \boldsymbol{b}_{23})$ is irrelevant for the computation of A_3. Hence it is much more interesting to compare

$$F_3(b) = b^4 (e^{-\beta V_3(b,b,b)} - 1) g^3(b). \tag{21}$$

Such a quantity is reported in Fig. 4 and shows that the relevant region corresponds to $1 \lesssim b \lesssim 3$. Moreover, while $F_3(b)$ is mostly negative for polymers, we have $F_3(b) = 0$ for model M1a, and, even worse, $F_3(b) > 0$ for model M2a. Hence, the compressible model gives

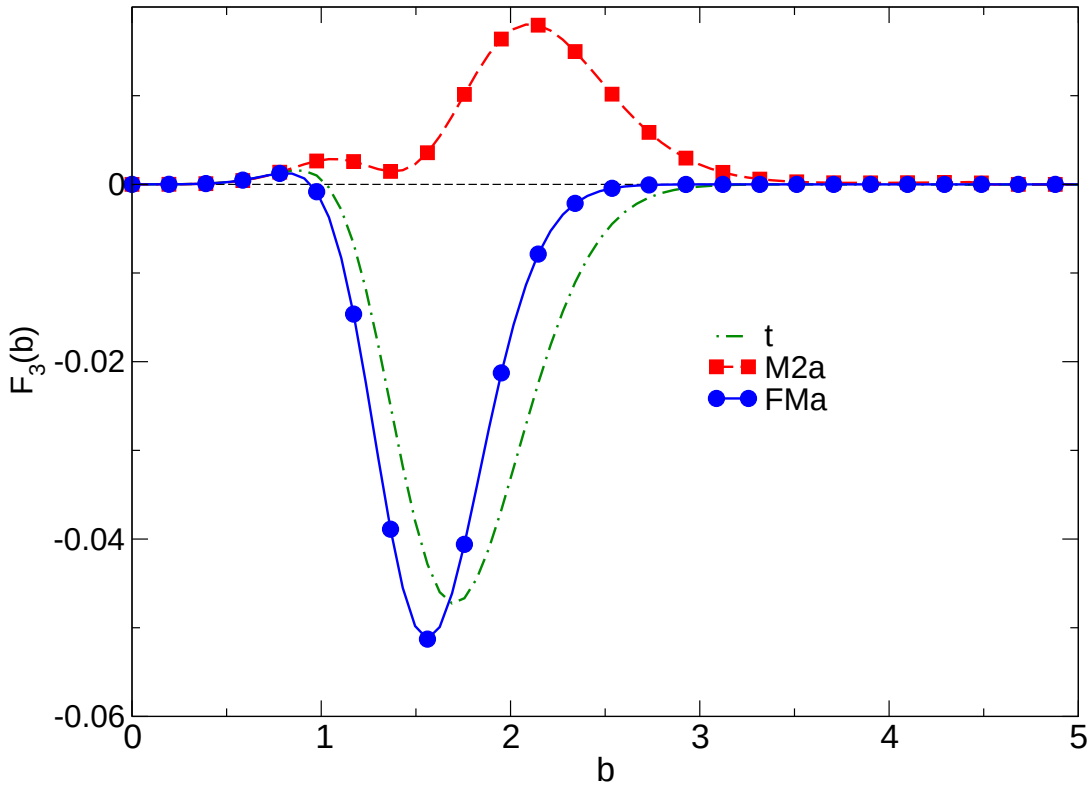

FIG. 4: Function $F_3(b)$ as a function of b, for polymers (FMa), for model M2a, and for the tetramer model of Ref. 22 (t).

a correction to the results for model M1a which has the wrong sign: hence, the discrepancy with the polymer results increases. For comparison, we also include the estimate of $F_3(b)$ for the tetramer model of Ref. 22, which is quite close to the polymer result, confirming that the tetramer model is a very good CG model in the dilute regime.

In Fig. 3 we also consider model M2b and the corresponding full monomer quantity (FMb). Potential FMb shows a clear logarithmic divergence as $b \to 0$, and indeed a general theoretical argument[9,38] predicts $V_3(b,b,b) \simeq -0.248\ln(1/b)$ for $b \to 0$. A fit of the small-distance data to $V_3 \simeq -0.248\ln(a/b)$ gives $a = 1.17$. The corresponding expression gives a good fit of the full-monomer data for V_3 up to $b \approx 0.9$. The three-body potential V_3 for model M2b is significantly different from the polymer one. For instance it is finite for $b \to 0$: $V_3(0,0,0) \approx -0.1$ for model M2b. Clearly, the CG model M2b is unable to correctly reproduce the three-body interactions.

TABLE II: Compressibility factor $Z(\Phi)$ for the models introduced in Sec. III, for the tetramer model (t) of Ref. 22, and for polymers (p) in the scaling limit.[41]

Φ	p	M1a	M1b	M2a	M2b	M2c	t
0.135	1.187	1.18458(1)	1.17869(1)	1.18455(1)	1.18090(1)	1.18630(1)	1.18993(4)
0.27	1.393	1.38167(1)	1.36439(1)	1.38084(2)	1.36758(1)	1.38379(2)	1.39852(6)
0.54	1.854	1.80067(1)	1.74840(1)	1.79770(2)	1.75010(2)	1.80119(2)	1.8499(1)
0.81	2.371	2.23911(1)	2.14190(1)	2.23498(2)	2.13765(2)	2.23694(2)	
1.09	2.959	2.70461(1)	2.55534(1)	2.70088(2)	2.54008(2)	2.69982(2)	2.9090(1)
2.18	5.634	4.55607(2)	4.18703(1)	4.56959(4)	4.08443(5)	4.55094(3)	5.2660(2)
4.36	12.23	8.29709(2)	7.47886(3)	8.36007(5)	6.9679(1)	8.31841(4)	10.2056(1)

B. The semidilute regime

We now analyze the behavior of the models in the semidilute regime. For this purpose we have performed simulations of the CG models for several values of the polymer volume fraction

$$\Phi = \frac{4\pi}{3} \hat{R}_g^3 c, \tag{22}$$

where $c = L/V$ is the number of polymers per unit volume. We have determined the compressibility factor $Z = \beta P/c$, the inverse compressibility $K = \partial(cZ)/\partial c$, the finite-density adimensional distribution $P(\sigma, \Phi)$ of r_g ($\sigma = r_g/\hat{R}_g$ as before), and the ratio $S_g(\Phi) = R_g^2(\Phi)/\hat{R}_g^2$. The compressibility factor was computed by using the molecular virial route[39,40] and checked by comparing it with the (significantly less precise) result obtained by using the compressibility route (we compute K as described in Ref. 41). Both methods give the same results within errors, confirming our final estimates. For models M1a and M1b we checked the Monte Carlo results using integral-equation methods— the hypernetted chain closure[14] for model M1a and the Rogers-Young closure[42] for model M1b: we found very good agreement, indicating that these methods are very accurate for these soft-sphere models.

In Table II and Fig. 5 we compare the estimates of Z for the different models. It is evident that considering radii dependent potentials is irrelevant for the thermodynamics, as already observed in the discussion of A_3: models M1a, M2a, and M2c give completely equivalent estimates and so do models M1b and M2b. Second, the CG model which uses the center of

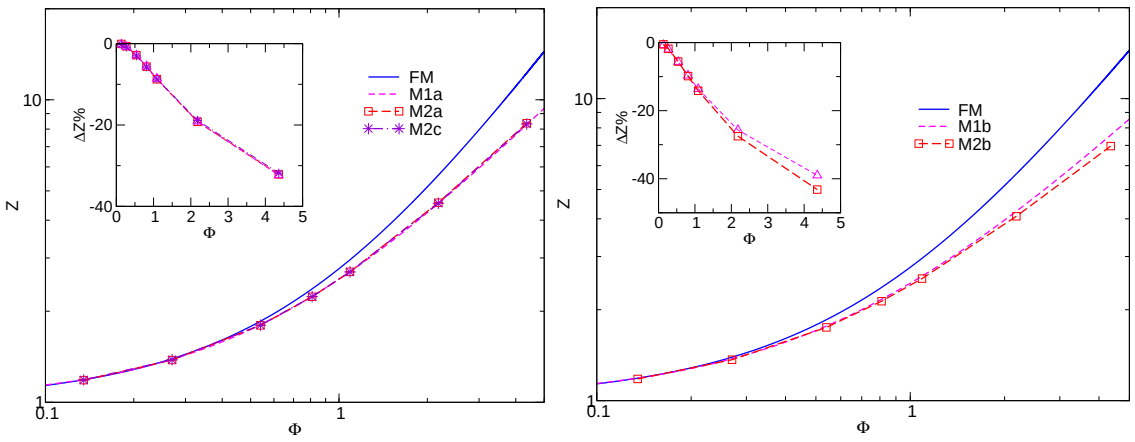

FIG. 5: Compressibility factor Z as a function of Φ. On the left we report results for models M1a, M2a, M2c, on the right we report the results for models M1b, M2b. They are compared with the polymer prediction Z_{FM} (full line, FM) (from Ref. 41). In the insets we report the deviations $100(Z/Z_{FM} - 1)$.

mass as reference point appears to be more accurate than that using the central monomer. For $\Phi = 1.09$, which is the expected boundary of applicability of single-blob models, models M1a and M2a predict Z with an error of 9%, while model M2b underestimates Z by 14%.

It is also interesting to compare the intermolecular distribution functions. In Fig. 6 we report the center-of-mass pair distribution function $g_{CM}(b)$ and the polymer-midpoint pair distribution function $g_{MP}(b)$. In the center-of-mass case (left panel) all results are in reasonable agreement for $b \gtrsim 1$, while larger discrepancies are observed for $b \to 0$. For the midpoint distribution all models give similar curves, even for small values of b. This is due to the logarithmic divergence of the potentials, which enforces the condition $g_{MP}(b) \to 0$ for $b \to 0$ in all models.

Finally, in Fig. 7 we report the distribution of the radius of gyration in the semidilute regime. For $\Phi = 1.09$ both types of coarse-graining reproduce correctly the polymer distribution of r_g. For $\Phi = 4.36$ deviations are significantly larger. However, this should not be considered as a problem of the method, but rather as consequence of the single-blob model, which is only expected to work in the dilute regime. To perform a more quantitative comparison we consider the ratio

$$S_g(\Phi) = \langle r_g^2 \rangle_\Phi / \hat{R}_g^2, \tag{23}$$

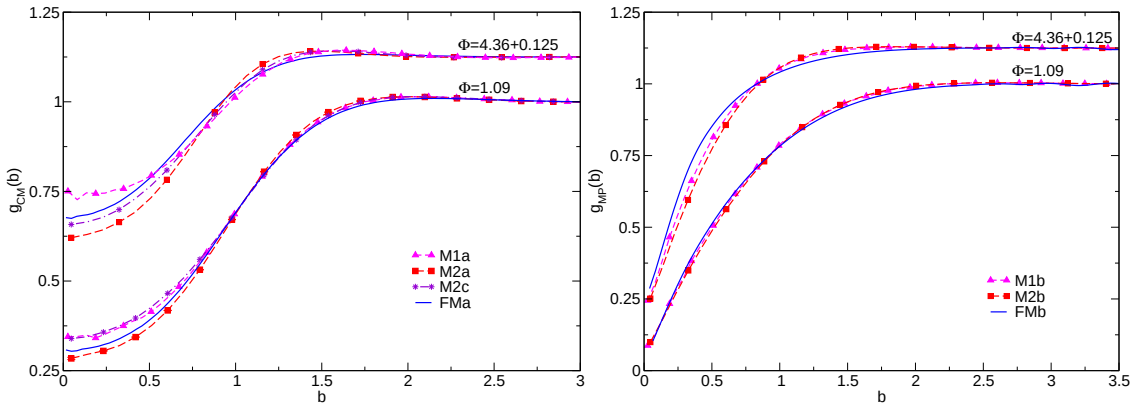

FIG. 6: Intermolecular distribution function for several models at $\Phi = 1.09$ and 4.36 (the corresponding function is shifted upward for clarity). On the left we report results for models M1a, M2a, M2c, and the polymer center-of-mass distribution from full-monomer simulations (FMa); on the right we report the results for models M1b, M2b, and the polymer distribution function associated with the polymer midpoint (FMb).

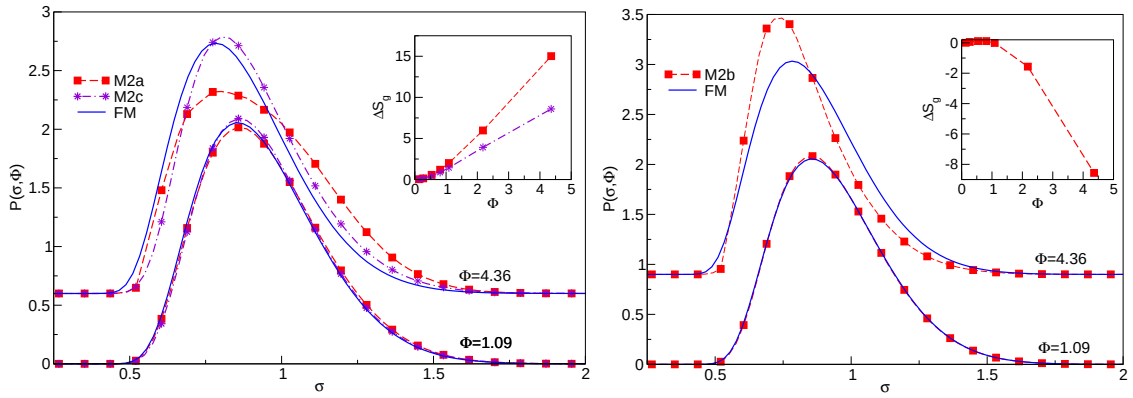

FIG. 7: Distribution $P(\sigma, \Phi)$ of $\sigma = r_g/\hat{R}_g$ for $\Phi = 1.09$ and 4.36 for CG models M2a, M2b, and M2c and for polymers (FM). In the insets we report the deviations $\Delta S_g = 100(S_g/S_{g,FM} - 1)$, where S_g is the ratio (23) for the CG models and $S_{g,FM}$ is the corresponding quantity for polymers.

where the average is performed at polymer volume fraction Φ. For $\Phi = 1.09$ we obtain $S_g(\Phi) = 0.94161(5)$ (M2a), 0.92300(6) (M2b), 0.93630(6) (M2c), to be compared with the polymer result $S_g(\Phi) = 0.9238(2)$. In all cases differences are small, although model M2b appears to reproduce better the polymer results. For larger values of Φ discrepancies increase, see the insets in Fig. 7, but this is not surprising for a single-blob model.

IV. CONCLUSIONS

In this paper we have performed a detailed study of single-blob models[21] which are characterized by a fluctuating sphere radius and by density-independent potentials which are such to reproduce the radius-of-gyration distribution for an isolated polymer and the center-of-mass (or midpoint) polymer distribution function in the limit of zero polymer density. The results have been compared with those obtained in simpler single-blob models with fixed blob radius with the purpose of understanding if CG models based on compressible blobs provide a more accurate description of the thermodynamic behavior than fixed-radius CG models. Since we use single-blob models, this comparison can only be made in the dilute regime $\Phi \lesssim 1$, in which polymer overlaps are rare.

As far as the thermodynamics and the intermolecular structure are concerned, we find that CG models that use the radii-dependent potentials behave no better than those in which polymers are represented by fixed-size spheres. However, the models with compressible soft spheres allow one to reproduce correctly (at least in the dilute regime in which single-blob models are expected to be predictive) the density dependence of the radius of gyration. For this quantity, the midpoint representation gives more accurate results.

The fact that models with fluctuating sphere size and models with fixed sphere size have the same thermodynamic behavior is probably related to the fact that the radius of gyration is not the relevant length scale at finite density. If one wishes to improve the accuracy of the model, one should take into account overlaps which are characterized by a different length scale, the de Gennes-Pincus correlation length ξ, which scales as $\xi \sim R_g \Phi^{-\gamma}$ with $\gamma = \nu/(3\nu - 1) \approx 0.77$ in the semidilute limit.[1–4] To describe the semidilute regime, only multiblob approaches appear to be viable coarse-graining methods. In this respect, on the basis of the present results, we do not expect the approach of Vettorel *et al.*[21] to be more accurate for the thermodynamics than the more straightforward approach of Refs. 17,22: considering compressible soft blobs should not provide a model which gives a more accurate description of the polymer thermodynamics than those in which the blob size is fixed. Indeed, both representations equally fail to take into account blob overlaps. Of course, a compressible soft-blob model would reproduce better the density dependence of some structural properties, like the average radius of gyration and the form factor.

One of the difficulties of multiblob approaches is the determination of the intra- and

inter-molecular potentials.[17,19,22] For models with compressible blobs, a direct numerical determination appears unfeasible, hence phenomenological approaches must be used. Ref. 21 proposed a simple parametrization for the intermolecular blob potential, Eq. (10). For the single-blob case we find that this parametrization is quite accurate: model M2c is essentially equivalent to model M2a.

Finally, we have compared the results for two different types of CG models. As for the thermodynamics, CG models for linear polymers that use the center of mass as reference point are significantly better than those that use the central monomer. Indeed, the estimates of the third virial coefficient and of the compressibility factor corresponding to models M1a and M2a are significantly closer to the full-monomer estimates than those obtained by using models M1b and M2b.

Acknowledgements

C.P. is supported by the Italian Institute of Technology (IIT) under the SEED project grant number 259 SIMBEDD Advanced Computational Methods for Biophysics, Drug Design and Energy Research.

Appendix A: Explicit expression for the third virial coefficient

In this Appendix we wish to derive an expression for the third virial coefficient which explicitly depends on the three-body potential of mean force defined in Eq. (19). We consider a generic system of molecules with internal degrees of freedom and on each molecule we select a reference point S. Then, we indicate with $\langle\cdot\rangle_{\mathbf{r}}$ the average over all internal degrees of freedom of the molecule such that the position of point S is $\mathbf{r}$. The formalism can be applied both to polymers — in this case the average is over all polymer conformations and S can be taken as the polymer center of mass or the central monomer — and to the single-blob CG model — in this case S is the position of the sphere and the average is over all values of its radius. Analogously, we define $\langle\cdot\rangle_{\mathbf{r}_1,\mathbf{r}_2}$ as the average over all additional degrees of freedom of two isolated molecules such that S_1 is in $\mathbf{r}_1$ and S_2 is in $\mathbf{r}_2$, and similar expressions involving three molecules. Finally, we define the zero-density S-related pair distribution function

$$g_S(r) = \langle e^{-\beta U_{12}} \rangle_{\mathbf{0},\mathbf{r}}, \tag{A1}$$

where U_{12} is the intermolecular potential energy, and the corresponding correlation function

$$h_S(r) = g_S(r) - 1 = \langle e^{-\beta U_{12}} - 1 \rangle_{\mathbf{0},\mathbf{r}} = \langle f_{12} \rangle_{\mathbf{0},\mathbf{r}}, \tag{A2}$$

where f_{12} is the usual Mayer function.

The third virial coefficient B_3 for the model can be written as[27]

$$B_3 = -\frac{1}{3} I_3 - T_1, \tag{A3}$$

where

$$\begin{aligned} I_3 &= \int d^3\mathbf{r}_{12} d^3\mathbf{r}_{13} \langle f_{12} f_{13} f_{23} \rangle_{\mathbf{0},\mathbf{r}_{12},\mathbf{r}_{13}}, \\ T_1 &= \int d^3\mathbf{r}_{12} d^3\mathbf{r}_{13} \left(\langle f_{12} f_{13} \rangle_{\mathbf{0},\mathbf{r}_{12},\mathbf{r}_{13}} - \langle f_{12} \rangle_{\mathbf{0},\mathbf{r}_{12}} \langle f_{13} \rangle_{\mathbf{0},\mathbf{r}_{13}} \right). \end{aligned} \tag{A4}$$

Using definition (19) we can rewrite

$$\begin{aligned} \langle f_{12} f_{13} f_{23} \rangle_{\mathbf{0},\mathbf{r}_{12},\mathbf{r}_{13}} &= \left(e^{-\beta V_3(\mathbf{r}_{12},\mathbf{r}_{13},\mathbf{r}_{23})} - 1 \right) g_S(r_{12}) g_S(r_{13}) g_S(r_{23}) \\ &+ h_S(r_{12}) h_S(r_{13}) h_S(r_{23}) \\ &- \left(\langle f_{12} f_{13} \rangle_{\mathbf{0},\mathbf{r}_{12},\mathbf{r}_{13}} - h_S(r_{12}) h_S(r_{13}) + 2 \text{ permutations} \right), \end{aligned} \tag{A5}$$

where $\mathbf{r}_{23} = \mathbf{r}_{13} - \mathbf{r}_{23}$ and the two permutations correspond to replacing once 13 with 23 and the second time 12 with 23. Using this expression we end up with

$$\begin{aligned} B_3 &= -\frac{1}{3} \int d^3\mathbf{r}_{12} d^3\mathbf{r}_{13} \left(e^{-\beta V_3(\mathbf{r}_{12},\mathbf{r}_{13},\mathbf{r}_{23})} - 1 \right) g_S(r_{12}) g_S(r_{13}) g_S(r_{23}) \\ &- \frac{1}{3} \int d^3\mathbf{r}_{12} d^3\mathbf{r}_{13} h_S(r_{12}) h_S(r_{13}) h_S(r_{23}). \end{aligned} \tag{A6}$$

It is interesting to observe that this expression is identical to the one which applies to a system of monoatomic molecules (without additional degrees of freedom) interacting by means of a two-body and of a three-body potential.

Using Eq. (A6) we can compute the difference $B_{3,\mathrm{pol}} - B_{3,CG}$ of the third virial coefficient for polymers and for the CG model. Since the S-related pair distribution function is, by definition, the same in the two models, the difference is given by Eq. (20) reported in the main text with $g(r) = g_S(r)$.

---

* Electronic address: giuseppe.dadamo@aquila.infn.it

† Electronic address: andrea.pelissetto@roma1.infn.it

‡ Electronic address: carlo.pierleoni@aquila.infn.it

[1] P. G. de Gennes, *Scaling Concepts in Polymer Physics* (Cornell University Press, Ithaca, NY, 1979).

[2] M. Doi, *Introduction to Polymer Physics* (Clarendon Press, Oxford, 1992).

[3] J. des Cloizeaux and G. Jannink, *Polymers in Solutions. Their Modelling and Structure* (Clarendon Press, Oxford, 1990).

[4] L. Schäfer, *Excluded Volume Effects in Polymer Solutions* (Springer, Berlin, 1999).

[5] C. N. Likos, Phys. Rep. **348**, 267 (2001).

[6] M. Dijkstra, R. van Roij, and R. Evans, Phys. Rev. E **59**, 5744 (1999).

[7] A. Y. Grosberg, P. G. Khalatur, and A. R. Khokhlov, Makromol. Chem., Rapid Commun. **3**, 709 (1982).

[8] J. Dautenhahn and C. K. Hall, Macromolecules **27**, 5399 (1994).

[9] C. von Ferber, A. Jusufi, C. N. Likos, H. Löwen, and M. Watzlawek, Eur. Phys. J. E **2**, 311 (2000).

[10] P. G. Bolhuis, A. A. Louis, and J. P. Hansen, Phys. Rev. E **64**, 021801 (2001).

[11] A. A. Louis, P. G. Bolhuis, J. P. Hansen, and E. J. Meijer, Phys. Rev. Lett. **85**, 2522 (2000).

[12] P. G. Bolhuis, A. A. Louis, J. P. Hansen, and E. J. Meijer, J. Chem. Phys. **114**, 4296 (2001); A. A. Louis, P. G. Bolhuis, R. Finken, V. Krakoviack, E. J. Meijer, and J. P. Hansen, Physica A **306**, 251 (2002).

[13] P. G. Bolhuis, A. A. Louis, and J. P. Hansen, Phys. Rev. Lett. **89**, 128302 (2002).

[14] J. P. Hansen and I. McDonald, *Theory of Simple Liquids*, 3rd ed. (Academic Press, Amsterdam, 2006)

[15] F. H. Stillinger, H. Sakai, and S. Torquato, J. Chem. Phys. **117**, 288 (2002).

[16] A. A. Louis, J. Phys.: Condens. Matter **14**, 9187 (2002).

[17] C. Pierleoni, B. Capone, and J. P. Hansen, J. Chem. Phys. **127**, 171102 (2007).

[18] D. Fritz, V. A. Harmandaris, K. Kremer, and N. F. A. van der Vegt, Macromolecules **42**, 7579 (2009).

[19] A. Pelissetto, J. Phys.: Condens. Matter **21**, 115108 (2009).

[20] A. J. Clark and M. G. Guenza, J. Chem. Phys. **132**, 044902 (2010).

[21] T. Vettorel, G. Besold, and K. Kremer, Soft Matter **6**, 2282 (2010).

[22] G. D'Adamo, A. Pelissetto, and C. Pierleoni, Soft Matter **8**, 5151 (2012).

[23] G. D'Adamo, A. Pelissetto, and C. Pierleoni, arXiv:1201.4275.

[24] M. Murat and K. Kremer, J. Chem. Phys. **108**, 4340 (1998).

[25] F. Eurich and P. Maass, J. Chem. Phys. **114**, 7655 (2001).

[26] N. Clisby, Phys. Rev. Lett. **104**, 55702 (2010).

[27] S. Caracciolo, B. M. Mognetti, and A. Pelissetto, J. Chem. Phys. **125**, 094903 (2006).

[28] N. Madras and A. D. Sokal, J. Stat. Phys. **50**, 109 (1988); T. Kennedy, J. Stat. Phys. **106**, 407 (2002); N. Clisby, J. Stat. Phys. **140**, 349 (2010).

[29] In the low-density limit the (osmotic) pressure Π of a polymer solution has an expansion of the form $\Pi/k_BT = c + B_2c^2$, where $c = L/V$ is the number of polymers per unit volume. The combination $A_2 = B_2\hat{R}_g^3$ is universal.

[30] C. N. Likos, H. Löwen, M. Watzlawek, B. Abbas, O. Jucknischke, J. Allgaier, and D. Richter, Phys. Rev. Lett. **80**, 4450 (1998).

[31] M. Watzlawek, C. N. Likos, and H. Löwen, Phys. Rev. Lett. **82**, 5289 (1999).

[32] A. Jusufi, J. Dzubiella, C. N. Likos, C. von Ferber, and H. Löwen, J. Phys.: Condens. Matter **13**, 6177 (2001).

[33] J. Dzubiella, C. N. Likos, and H. Löwen, J. Chem. Phys. **116**, 9518 (2002).

[34] T. A. Witten and P. A. Pincus, Macromolecules **19**, 2509 (1986).

[35] H.-P. Hsu and P. Grassberger, Europhys. Lett. **66**, 874 (2004).

[36] The potential is parametrized as (Ref. 37) $V(b) = \sum_i a_i e^{-b^2/c_i^2}$, $i = 1, 2, 3$, with $a_1 = 0.999225$, $a_2 = 1.1574$, $a_3 = -0.38505$, $c_1 = 1.24051$, $c_2 = 0.85647$, and $c_3 = 0.551876$.

[37] A. Pelissetto and J.-P. Hansen, J. Chem. Phys. **122**, 134904 (2005).

[38] A. Pelissetto, Phys. Rev. E **85**, 021803 (2012).

[39] G. Ciccotti and J. P. Ryckaert, Comp. Phys. Rep. **4**, 346 (1986).

[40] R. L. C. Akkermans and G. Ciccotti, J. Phys. Chem. B **108**, 6866 (2004).

[41] A. Pelissetto, J. Chem. Phys. **129**, 044901 (2008).

[42] F. A. Rogers and D.A. Young, Phys. Rev. A **30**, 999 (1984).